Exploring the diffusion of charm quarks in a deconfined medium by Color String Percolation approach

M.Sc. Thesis

by

Kangkan Goswami

DEPARTMENT OF PHYSICS

INDIAN INSTITUTE OF TECHNOLOGY INDORE

June 2021

Exploring the diffusion of charm quarks in a deconfined medium by Color String Percolation approach

A THESIS

Submitted in partial fulfillment of the requirements for the award of the degree of

Master of Science

by

Kangkan Goswami

under the guidance of

Dr. Raghunath Sahoo

DEPARTMENT OF PHYSICS

INDIAN INSTITUTE OF TECHNOLOGY INDORE

June 2021

INDIAN INSTITUTE OF TECHNOLOGY INDORE

CANDIDATE'S DECLARATION

I hereby certify that the work which is being presented in the thesis entitled **"Exploring the diffusion of charm quarks in a deconfined medium by Color String Percolation approach"** in the partial fulfillment of the requirements for the award of the degree of **MASTER OF SCIENCE** and submitted in the **Department of Physics, Indian Institute of Technology Indore**, is an authentic record of my own work carried out during the time period from August 2020 to June 2021 under the supervision of Dr. Raghunath Sahoo, Associate Professor, Indian Institute of Technology Indore.

The matter presented in this thesis has not been submitted by me for the award of any other degree of this or any other institute.

18.06.2021

Signature of the student with date

(Kangkan Goswami)

This is to certify that the above statement made by the candidate is correct to the best of my knowledge.

18.06.2021

Signature of the Supervisor of M.Sc. thesis(with date)

(Dr. Raghunath Sahoo)

Kangkan Goswami has successfully given his M.Sc. Oral Examination held on **June 18, 2021**.

18/06/2021

Signature of Supervisor of M.Sc. thesis
Date:

24-06-2021

Convener, DPGC
Date:

Signature of PSPC Member 1
Date: 18.06.2021

Signature of PSPC Member 2
Date: 19/6/21

ACKNOWLEDGEMENTS

Foremost, I would like to express my sincere gratitude to my advisor Dr. Raghunath Sahoo for his continuous support during my M.Sc. project, patience, motivation, and immense knowledge. His guidance helped me in all the time of research, studying, and writing of this thesis.

Besides my advisor, I would like to thank my PSPC committee members: Prof. Subhendu Rakshit and Dr. Debajyoti Sarkar for their support and encouragement. I am very grateful to the Physics Department of IIT Indore for providing me all the required facilities.

I am thankful to my fellow labmates of the Experimental High-Energy Physics group at IIT Indore. I can't express enough thanks to Dushmanta Sahu who was of immense help during the project. He helped with everything, from all kinds of physics problems to technical problems in LaTeX and ROOT. I would also like to thank Dr. Captain Rituraj Singh for his help and insightful comments. All the discussions we had helped me to stay motivated and work harder.

Kangkan Goswami

Dedicated to my parents.

Abstract

We have studied relativistic heavy-ion collisions using Color String Percolation Model. We have estimated hadronization temperature and studied the diffusion of charm quarks in a deconfined medium. Estimation of drag and diffusion coefficients has been done by using the Fokker-Planck equation considering the heavy quarks in Brownian motion. We have studied the variation of drag and diffusion coefficients with temperature. As temperature increases, the system density increases, which results in a higher drag and transverse momentum diffusion coefficient. The study of spatial diffusion coefficient shows a decreasing trend first and then increases with temperature. A minima can be observed near hadronization temperature hinting at a possible phase transition.

Table of Contents

List of Figures

Chapter 1

Introduction

Everything around us is made up of atoms, which themselves are made up of further smaller elementary particles. Human curiosity and technological advancements have encouraged us to search for elementary particles. First, it was discovered that atoms are made up of protons, neutrons, and electrons. Soon it was realized that proton and neutron are a part of a bigger family, namely hadron, and electron was classified as a lepton. The theoretical framework of the standard model was developed incorporating all known elementary particles. Standard model consists of:

1. Three fundamental forces and their intermediary bosons.

2. Two classes of particles, quarks and leptons.

Three fundamental forces are the strong force, the weak force, and the electromagnetic force. The strong force acts at a range of order of 10^{-15} m and it rapidly decreases to insignificant values at higher distances. It acts as an attractive force to bind the quarks to form hadrons. The weak forces are responsible for nuclear beta decay as well as decay of pions, kaons and many of the strange particles. Electromagnetic forces are responsible for attractive and repulsive interactions between the charged particles. Intermediary bosons are gluons (act as a gauge boson for the strong interactions), $Z^0, W^\pm$ (act as intermediate bosons for weak interaction), and photons (act as an exchange particle in electromagnetic interaction). Quarks and leptons have their respective antiparticles (antiquarks and antileptons). These quarks, leptons, and their antiparticles are divided into three generations, the first one being the most stable and lightest. Like an electron that has a negative electric charge of one unit, a quark also has an electric charge of either $+\frac{2}{3}$e or $-\frac{1}{3}$e. But along with the electric charge, it also has a color charge that can come in three categories red, blue or green. Antiquarks have color charges; anti-red, anti-blue, and anti-green.

Baryons and mesons are composite particles, collectively known as hadrons, and are made up of three quarks (qqq) and a quark and an antiquark ($q\bar{q}$) respectively. These are color charge-neutral particles. As only color-neutral particles can exist in nature due to color confinement, the quarks are always confined in the form of mesons and baryons. The quarks and their behavior can be studied using Quantum Chromo Dynamics (QCD). According to QCD, the strength of the coupling constant (α_s) decreases with energy and increases with distance. This behavior is termed asymptotic freedom. Theoretically, deconfined quarks are to be found above temperatures above the hadronization temperature. For the exploration of deconfined matter and to achieve extreme temperatures, particles were accelerated with higher and higher energies at laboratories like Relativistic Heavy Ion Collider (RHIC)

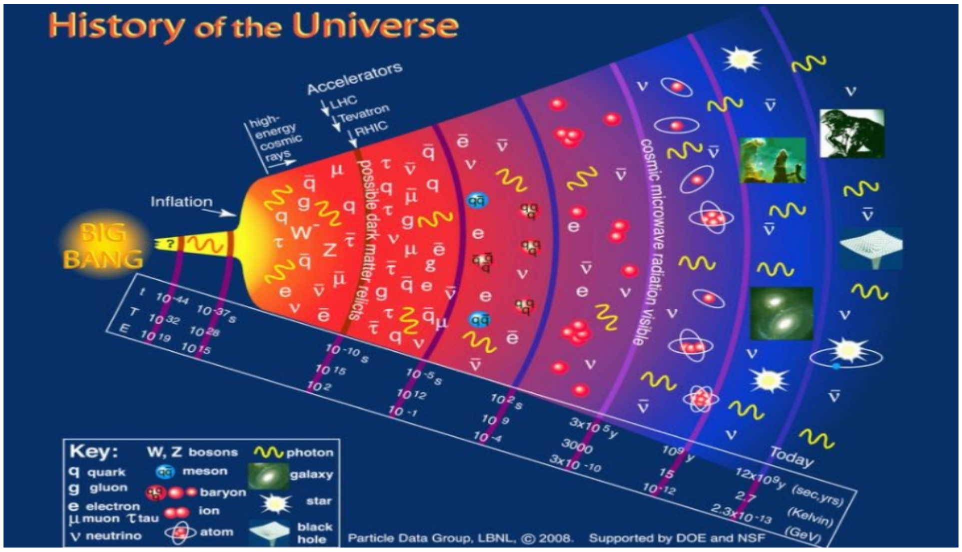

Figure 1.1: Expanding Universe [1]

and the Large Hadron Collider (LHC).

1.1 Relativistic Heavy Ion Collision

The universe that we observe now has expanded from an initial extremely dense and hot state of matter, where quarks and gluons are assumed to have existed freely. This state of deconfined quarks and gluons formed within the first few microseconds (10^{-6} seconds) after the Big Bang when the temperature was estimated to be the order of 10^{12}K. With time, the produced matter expanded and cooled down and eventually the deconfined quarks and gluons hadronized. Further, these hadrons formed atomic nuclei and everything that we see around us today.

To understand the matter formed in the early universe, scientists have taken advantage of ultra-relativistic hadronic and nuclear collisions. Scientists in RHIC and LHC are accelerating particles close to the speed of light. Mathematically, the energy of these particles is given as E = γm, where γ is the Lorentz factor which increases with increasing velocity. At the LHC, the energy of the colliding particles has reached up to TeV energies. With this increase in energy, the temperature of the produced matter increases to such an extent that the quarks and gluons in this state become deconfined, known as Quark gluon plasma (QGP).

For the production of QGP in a laboratory, we collide heavy-ions traveling with TeV energies. When two incoming particles collide, their overlapping parts interact strongly creating a dense and hot system of matter. Initially, the matter is in the deconfined phase, i.e. QGP. But with time, it expands and cools down and finally undergoes hadronization long before it reaches the detectors. So practically, we never directly detect QGP. But we can observe different signs of the formation of QGP from the detected final state hadrons. There are many probes to study QGP formation, namely strangeness enhancement, elliptic flow measurement, J/ψ suppression, and jet quenching.

1.2 Quark-Gluon Plasma (QGP)

QCD predicted that quarks and gluons are always confined in form of hadrons due to color confinement. However, due to asymptotic freedom, it was expected that deconfined quarks and gluons should exist freely at high temperatures or high baryon densities. To have better intuition, we can take an analogy of ionized gas where quarks and gluons are analogous to electrons and ions.

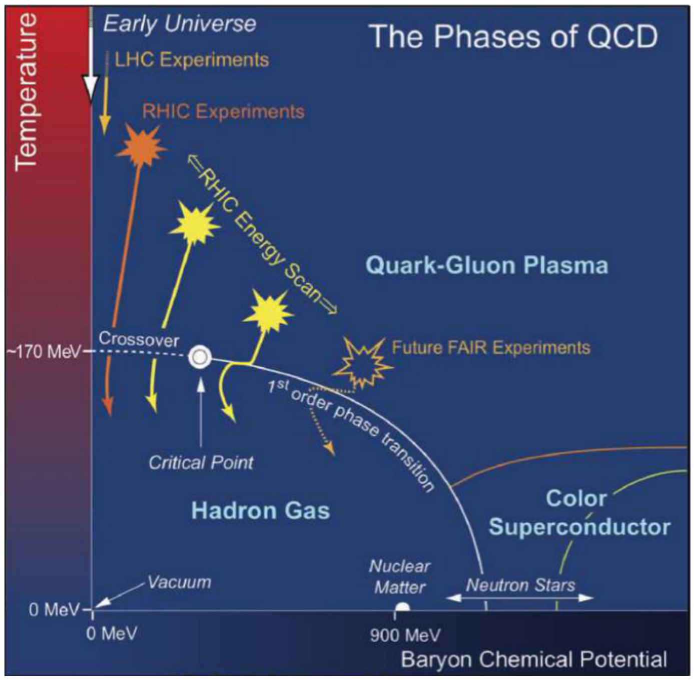

Figure 1.2: Phase diagram of QCD. [2]

In fig (1.2), different phases of QCD have been shown in a plot where the temperature has been plotted as a function of baryon chemical potential. Vacuum is taken as the origin with zero absolute temperature and zero baryon chemical potential. The early universe can be imagined as having a very high temperature with almost no baryon chemical potential. On other hand, stellar objects like neutron stars correspond to low temperature and very high baryon chemical potential.

RHIC and LHC experiments produce very high temperature and low baryon chemical potential creating a possibility of formation of QGP, undergoing a crossover phase transition from hadron gas.

The collision of relativistic heavy-ion leads to the production of deconfined quarks and gluons with high transverse momentum (p_T). These deconfined quarks and gluons thermalize ($\tau \sim 10$ fm/c) due to elastic and inelastic scattering among them. The system expands rapidly, while a few quarks and gluons undergo hadronization that gives rise to the mixed-phase. Then slowly the system expands and cools down further.

After a critical temperature, the whole system undergoes hadronization through fragmentation or coalescence. While coalescence dominates at low energy, fragmentation is the preferred mechanism for high energy partons. Due to further expansion, the inelastic collision between the hadrons ceases which in turn reduces the production of new hadrons. This freezes the particle ratio with time. This is known as chemical freeze-out.

It is predicted that after the chemical freeze-out, there is a phase transition from QGP to hadron gas. It can be studied by implementing a statistical hadron gas model. It ignores the interaction between hadrons. For better understanding, we can say that this phase is analogous to a system of an ideal gas. As the particles move towards the detector, the mean free path of the particles becomes larger than the system size. Due to this, the elastic collisions stop which in turn freezes the momentum distribution of the system. This phase is known as kinetic freeze-out.

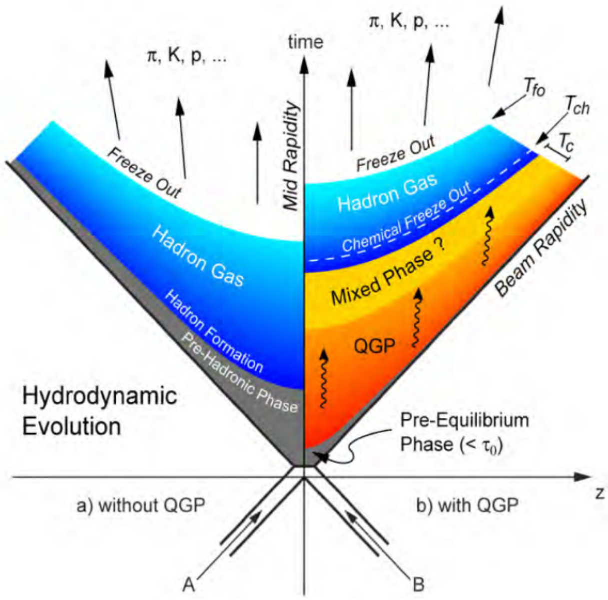

Figure 1.3: Possible space-time evolution of heavy-ion collision, with and without formation of QGP [3]

1.3 Detector Geometry

To mathematically treat a detected particle, we use the geometry shown in fig. (1.4) .Conventionally, the beamline is taken as the z-axis, or the longitudinal direction while the XY plane is taken as the transverse plane. Generally, the momentum of the produced particle is divided into two components, p_z, longitudinal momentum, and p_T, transverse momentum. Mathematically, it can be expressed as $p_T = \sqrt{p_x^2 + p_y^2}$. We are generally interested in the transverse momentum as there is no initial momentum along this plane. Thus the transverse component of momentum is originated solely due to the collision byproduct.

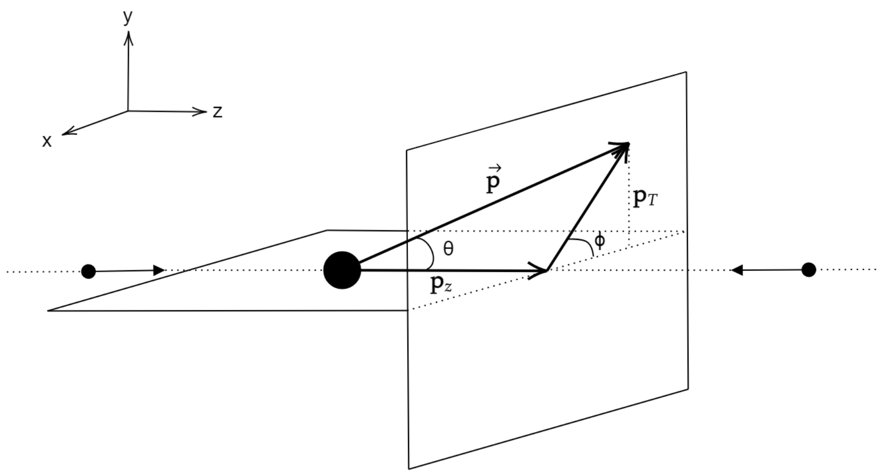

Figure 1.4: The decomposition of particle momentum into p_z and p_T components.

Polar angle (θ) is defined as the angle made by the momentum of the produced particle with the beam direction and mathematically it is given as,

$$\theta = \cos^{-1}\frac{p_z}{|\vec{p}|} = \tan^{-1}\frac{p_T}{p_z}$$

The azimuthal angle (ϕ) is defined as,

$$\phi = \tan^{-1}\frac{p_y}{p_x}$$

1.4 Relativistic Kinematics

Relativistic kinematics is used to study relativistic collisions, produced particles, and their dynamics, the formalism of relativistic kinematics is used. To fully understand and reconstruct the detected particles, many observables are needed to be calculated. For such calculations, we use natural units taking $\hbar = c = 1$.

1.4.1 Rapidity

In the case of Lorentz transformation, the velocity of the particles is not additive in nature. Thus we use a new variable that is additive in nature under successive Lorentz transformation, called rapidity. It is defined as

$$y = \frac{1}{2} \ln \left(\frac{1+\beta}{1-\beta} \right)$$

We can write, $\beta = \tanh y$, where $\beta = \frac{v}{c}$
For N successive Lorentz transformation, rapidity can be calculated as, $y = y_1 + y_2 + y_3 ... + y_N = \Sigma y_i$.
Rapidity for a particle with energy, E and longitudinal momentum p_z is given as,

$$y = \frac{1}{2} \ln \left(\frac{E+p_z}{E-p_z} \right)$$

where, $E = \sqrt{p_x^2 + p_y^2 + p_z^2 + m^2} = \sqrt{m^2 + p^2}$

1.4.2 Pseudorapidity

For a particle travelling with relativistic velocity, $p >> m$, that gives us $E = \sqrt{p^2 + m^2} \approx p$. We assume that the particle makes an angle θ with the beam axis (i.e. z-axis) such that $p_z = p\cos\theta$. The rapidity can be approximated as

$$y \approx \frac{1}{2}\ln\left(\frac{p + p\cos\theta}{p - p\cos\theta}\right) \approx -\ln\tan\frac{\theta}{2}$$

We define a new variable, pseudorapidity,(η).

$$\eta = -\ln\tan\frac{\theta}{2}.$$

Practically, pseudorapidity can be easily calculated, as any detector can easily measure the angle of the produced particle with respect to the beam axis. Moreover, to calculate pseudorapidity we do not need the energy or momentum information.

1.5 Motivation

The system created in the early stages of heavy-ion collision has been a point of interest for theoretical as well as experimental physicists. The deconfined quarks and gluons hadronize long before they reach the detectors. To have a better understanding of the produced deconfined matter, different models have been used to study the produced system.

In this work, we have used Color String Percolation Model (CSPM) to study the produced system. With its help, we can estimate the initial temperature and the initial energy density of any hadronic or nuclear collision system. Other thermodynamic and transport properties such as shear viscosity to entropy density ratio, mean free path, bulk viscosity to entropy density ratio can be estimated as well [4].

Heavy quarks (HQs) form in the initial stages of relativistic heavy-ion collision. The collision between HQs and a thermal quark changes the energy of the heavy quark only marginally, hence the thermal equilibrium time of heavy quarks is much larger as compared to the thermal equilibrium time of light quarks as well as the lifetime of QGP. As a result of this, the HQ witness the evolution of the formed hot and dense matter making it an effective probe to study the properties of QGP. Because of this reason, we want to study the diffusion of charm quark in a deconfined medium which will help us to obtain useful information about the medium formed in ultra-relativistic collisions.

Chapter 2

Color String Percolation Model (CSPM)

Color String Percolation Model is a QCD-inspired model. We use a simple 2D percolation example to study color string percolation. We randomly distribute discs of an area πr_0^2 on a larger surface such that the discs are allowed to overlap, where r_0 is the radius of a single disc. As the number of discs increases, they will start to overlap to form clusters. If we consider N such discs are distributed in a surface area S, the number density of discs is given as $\rho = N/S$. At some critical density (ρ_c), the clusters span the whole system marking the percolation phase transition.

We can take $N \to \infty$ with fixed ρ, then from Poissonian distribution

$$P_n = \frac{\xi^n}{n!} exp(-\xi)$$

with mean ξ, can be used be describe the overlapping of discs such that $\xi = \rho\pi r_0^2$, where r_0 is the radius of a disc.

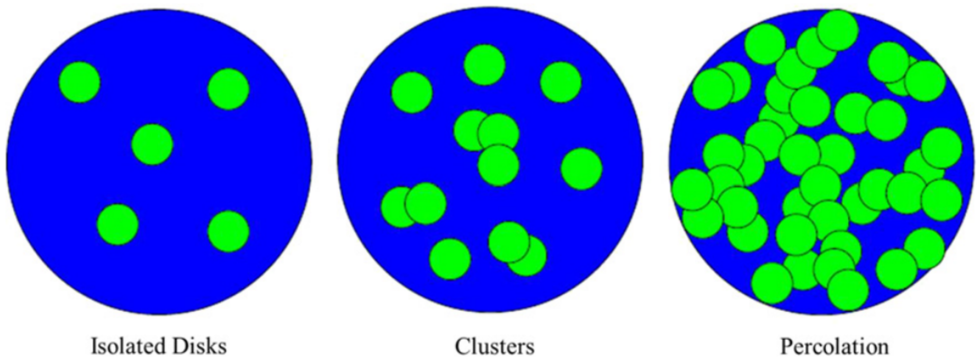

Figure 2.1: Isolated discs, cluster formation and percolation phase transition [5]

In this model, the production of particles can be understood as color strings stretching between the colliding target and projectile. Subsequently, the string breaks which leads to the formation of quark-antiquark pair. If we assume that S_1 is the transverse area of a single string, then the percolation density parameter is given as $\rho = N\frac{S_1}{S_N}$, where S_N is the total transverse overlap area.

We assume that N strings form clusters that span the whole transverse area with an area of S_N. It behaves as a single color source with color field $\vec{Q_N}$, which can be taken as the superposition of color field of every single string such that $\vec{Q_N} = \sum_{i=1}^{N} \vec{Q_1}$. On obtaining $\vec{Q_N}$, we calculate multiplicity (μ) and mean transverse momentum squared ($\langle p_T^2 \rangle$) of the produced particles from N strings [6],

$$\mu_N = \sqrt{\frac{NS_N}{S_1}}\mu_0; \quad \langle p_T^2 \rangle_N = \sqrt{\frac{NS_1}{S_N}}\langle p_T^2 \rangle_1 \tag{2.1}$$

where, μ_0 and $\langle p_T^2 \rangle_1$ are the multiplicity and mean transverse momentum squared produced from a single string. In the thermodynamic limit, i.e. $N \to \infty$, we get the following expression [6, 7],

$$\langle \frac{NS_1}{S_N} \rangle = \frac{\xi}{1 - e^{-\xi}} = \frac{1}{F(\xi)^2}$$

or, we can write $F(\xi)$ as,

$$F(\xi) = \sqrt{\frac{1 - e^{-\xi}}{\xi}} \tag{2.2}$$

where $F(\xi)$ is the color suppression factor. We can write multiplicity of produced paticles from N strings as $\mu_N = NF(\xi)\mu_0$ and mean transverse momentum squared can be written as $\langle p_T^2 \rangle_N = \langle p_T^2 \rangle_1 / F(\xi)$.

2.1 Color Suppression Factor, $F(\xi)$

$F(\xi)$ can be estimated from the experimental data by fitting the transverse momentum spectra of charged particles from pp and A-A collisions at different centralities and different energies.

To determine the initial ξ, we use the experimental data from pp collisions at $\sqrt{s} = 200$ GeV by fitting it with [8],

$$\frac{d^2 N_{ch}}{dp_T^2} = \frac{a}{(p_0 + p_T)^{\alpha}} \tag{2.3}$$

where, a is the normalization factor and p_0 and α are the fitting parameters given as $p_0 = 1.982$ and $\alpha = 12.877$.

For high multiplicity pp and heavy-ion collisions, we can use this parameterisation by changing the parameter p_0 as [9],

$$p_0 \to p_0 \left(\frac{\langle N_S S_1 / S_N \rangle_{pp,pA,AA}}{\langle N_S S_1 / S_N \rangle_{pp,\sqrt{s}=200GeV,}} \right) \tag{2.4}$$

For high multiplicity pp, pA and AA collisions, we can write [2.3] as,

$$\frac{d^2N_{ch}}{dp_T^2} = \frac{a}{\left(p_0\sqrt{\frac{F(\xi)_{pp,\sqrt{s}=200GeV}}{F(\xi)_{pp,pA,AA}}} + p_T\right)^{\alpha}} \tag{2.5}$$

In low energy pp collision, $F(\xi)_{pp} \sim 1$, due to low string overlap probability.

2.2 CSPM Observables

2.2.1 Temperature

The temperature of the produced system can be expressed as in terms of F(ξ). It involves the Schwinger mechanism for particle production. The Schwinger distribution for massless particles can be expressed in terms of p_T^2 as [10, 11],

$$\frac{dn}{dp_T^2} \sim exp\left(-\frac{\pi p_T^2}{x^2}\right)$$

where $\langle x^2\rangle$ is the average value of string tension. As the chromo-electric field is not constant, the tension of the macroscopic cluster fluctuates around its mean value. Due to these fluctuations, we get a Gaussian distribution of the string tension that can be written as,

$$\frac{dn}{dp_T^2} \sim \sqrt{\frac{2}{\langle x^2\rangle}}\int_0^\infty dx\;\; exp\left(-\frac{x^2}{2\langle x^2\rangle}\right) exp\left(-\pi\frac{p_T^2}{x^2}\right)$$

It gives rise to a thermal distribution [12],

$$\frac{dn}{dp_T^2} \sim exp\left(-p_T\sqrt{\frac{2\pi}{\langle x^2\rangle}}\right)$$

where $\langle x^2 \rangle = \pi \langle p_T^2 \rangle_1 / F(\xi)$

The temperature in terms of F(ξ) is given as [13, 14],

$$T(\xi) = \sqrt{\frac{\langle p_T^2 \rangle_1}{2F(\xi)}} \tag{2.6}$$

where $\langle p_T^2 \rangle_1$ is the average transverse momentum squared of a single string. We get $\sqrt{\langle p_T^2 \rangle_1}$= 207.2 ± 3.3 MeV by taking the critical values ξ_c=1.2 and T_c = 167.7 ±2.8 MeV [15].

2.2.2 Shear Viscosity to entropy density ratio

The ratio of shear viscosity to entropy density ratio can be taken as a measure of the fluidity of the system, which can act as an important observable to understand the produced matter. According to AdS/CFT calculations, η/s have a lower bound of $1/4\pi$ [16].

Shear viscosity to entropy density ratio can be expressed as [4],

$$\frac{\eta}{s} \simeq \frac{T\lambda}{5} \tag{2.7}$$

where T is the temperature and λ is the mean free path. Mean free path can be expressed as [4],

$$\lambda = 1/(1 - e^{-\xi}) \tag{2.8}$$

Using above expression for mean free path, we obtain the expression for shear viscosity to entropy density ratio as,

$$\frac{\eta}{s} = \frac{TL}{5(1 - e^{-\xi})} \tag{2.9}$$

where, L is the longitudinal extension of the string ~ 1.

The shear viscosity is found to be temperature-dependent for the matter produced in the relativistic heavy-ion collision. It decreases on approaching the critical temperature. We can predict to observe the lowest value near critical temperature and it increases after hadronization. This can be explained as, below the critical percolation density (ξ_c), the string density increases with an increase in temperature. As the area is rapidly filled, the mean free path (λ) decreases sharply. From Eq.(2.7), we can predict that η/s will decrease sharply as well. On crossing ξ_c, we can say that more than 2/3 of the area is already filled by color string. Due to this, now the color string fills up the area at a decreased rate. This leads to a small decrease in the mean free path. The rising temperature compensates for this and we observe a smooth increase in shear viscosity to entropy density ratio.

The minima observed for shear viscosity to entropy density ratio around critical temperature suggest possible phase transition.

Chapter 3

Diffusion of charm quark

According to the Standard Model of particle physics, we have six quarks out of which three are considered heavy quarks: charm, bottom, and top. Fig. (3.1) depicts the relative heaviness of these quarks.

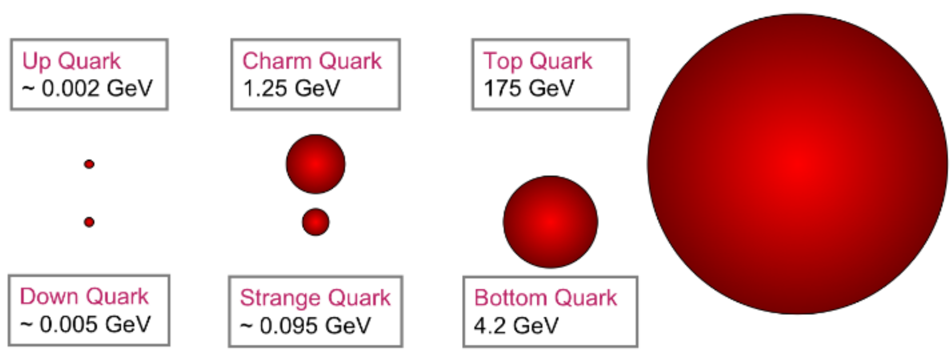

Figure 3.1: Size represents relative mass of each quark [17]

The production cross-section of the top quark is relatively low and it is very unstable due to its huge mass. It decays very fast into the bottom and charm quark. Due to their large masses, they are produced in the initial stages of the collision. Due to interaction with the QGP medium, the momentum spectra of the charm quarks get modified and it can be studied to understand the interaction. Although, this interaction doesn't thermalize the intermediate and high-p_T charm quarks. Charm quarks then undergo hadronization and reach the detector. The study of charm quarks can give us important information about the QGP medium and can be a very useful probe. Similarly, for investigating the hadron gas, many studies have been done on estimating the properties of D meson, which contains a charm quark along with a light quark.

It has been estimated that thermalization time for charm quarks are of order 10-15 fm/c and 25-30 fm/c for bottom quarks [18]. Lifetime of QGP is estimated to be order of 4-5 fm/c at RHIC [19] and 10-12 fm/c at LHC [20]. Thus, charm and bottom quarks are predicted to witness the evolution of the produced matter. They propagate through the QGP and interacts with the constituent particles.

In the QGP medium, the light quarks and gluons were thermalized early. Due to the interaction of heavy quarks with light quarks and gluons, the motion of these heavy quarks can be studied as Brownian motion and can be treated with some form of Boltzmann transport equation. Because of the large mass difference between charm, bottom, and other constituent particles of QGP, the Boltzmann equation reduces to the Fokker-Planck equation.

The interaction of charm quark with the medium can be studied quantitatively by studying the variation of drag and diffusion coefficient with temperature. In this study, we have estimated the drag and diffusion coefficient of charm quark propagating in the produced deconfined medium. As the charm quarks interact with the medium its average momentum changes, its momentum spectrum broadens. The drag and diffusion coefficient incorporates these changes.

Propagation of charm quarks in QGP medium have been studied using the Fokker-Planck equation given as [21],

$$\frac{\partial f(t,\mathbf{p})}{\partial t} = \frac{\partial}{\partial p_i}\{\gamma_i(\mathbf{p})f(t,\mathbf{p}) + \frac{\partial}{\partial p_j}\left[B_{ij}(\mathbf{p})f(t,\mathbf{p})\right]\} \tag{3.1}$$

where $f(t, \mathbf{p})$ is the distribution function of charm quark in medium. $\gamma(\mathbf{p})$ and $B(\mathbf{p})$ are the drag and momentum diffusion coefficient respectively. They are given as,

$$\gamma_i(\mathbf{p}) = \int d\mathbf{k}\ \omega(\mathbf{p},\mathbf{k})k_i$$

$$B_{ij}(\mathbf{p}) = \frac{1}{2}\int d\mathbf{k}\ \omega(\mathbf{p},\mathbf{k})k_i k_j$$

The drag coefficient (γ) accounts for average momentum change. The momentum diffusion (B_{ij}) incorporates the broadening of the final momentum distribution of the detected particles. The momentum diffusion coefficient can be further separated into two components such as the transverse (B_0) and longitudinal (B_1) momentum diffusion coefficient. The average momentum of a charm quark in this medium is given by,

$$\langle p\rangle = \frac{\int_{-}{}_{\infty}^{\infty} dp\ pf(t,p)}{\int_{-}{}_{\infty}^{\infty} dp\ f(t,p)}$$

$$\langle p\rangle = p_0\ exp\left(-\frac{t}{\tau_R}\right) \tag{3.2}$$

where τ_R is the relaxation time of charm quark. It is defined as the time required for the exponential decay of average momentum. For light quarks, relaxation time can be expressed as [22],

$$\tau \simeq 5\frac{\frac{\eta}{s}}{T} \tag{3.3}$$

For heavy quarks, we can write the expression for relaxation time as [23],

$$\tau_R = \frac{m_c}{T}\tau \tag{3.4}$$

where, $m_c = 1.275$ GeV is the mass of charm quark. According to CSPM formalism, using (2.9) and (3.3), we can express relaxation time for charm quark as,

$$\tau_R = \frac{m_c L}{T(1 - e^{-\xi})} \tag{3.5}$$

The drag coefficient is related to the relaxation time by [24],

$$\gamma = \frac{1}{\tau_R} \tag{3.6}$$

According to Einstein's relation, transverse diffusion momentum coefficient is [25],

$$B_0 = \gamma T(m_c + T) \tag{3.7}$$

Square of mean displacement of a particle in the medium after time t can be written as,

$$\langle (x(t) - x(0))^2 \rangle = 2D_s t$$

where D_s is the spatial diffusion coefficient. From the above equation, we can conclude that D_s can be used as a measure of the speed of diffusion of charm quarks in space. In static limit, it can be expressed as [21],

$$D_s = \frac{T}{m_c \gamma} \tag{3.8}$$

Chapter 4

Results and Discussions

In this work, as discussed above we have theoretically estimated the temperature obtained in a relativistic heavy-ion collision using the Color string percolation model. Different values of color suppression factor, $F(\xi)$, is taken to estimate percolation density parameter, (ξ), and temperature using Eq. (2.2) and (2.6). The results have been tabulated.

Here, we can observe that temperature increases with ξ, as the density increases from pp to heavy-ion collision, the initial temperature of the produced matter also increases with it. Around the critical percolation density parameter, $\xi_c = 1.2$, the estimated temperature is around 0.169 GeV, which is near the hadronization temperature.

The diffusion of charm quarks in the produced matter has been studied by estimating drag and diffusion coefficient. We have used Eq. (3.5) to calculate the relaxation time for the charm quarks and studied its variation with temperature. We found that relaxation time decreases with increasing temperature. This is because, at low temperature and low-density medium, the charm quark will interact with the lighter quarks less, which will result in a high relaxation time. As the system density increases, the charm quark will interact more with the lighter quarks, resulting in a low relaxation time. We observe that relaxation time for charm quarks is higher than the lifetime of produced QGP (~ 5 fm).

F(ξ)	ξ	Temperature (GeV)
0.90	0.44	0.1544
0.85	0.69	0.1589
0.80	0.97	0.1638
0.75	1.29	0.1691
0.70	1.65	0.1751
0.65	2.07	0.1817
0.60	2.64	0.1891
0.55	3.26	0.1975
0.50	4.04	0.2072
0.45	5.13	0.2184
0.40	6.56	0.2316
0.35	8.64	0.2476
0.30	11.89	0.2674
0.25	17.36	0.2931
0.20	27.70	0.3276
0.15	51.02	0.3782

The drag coefficient is related to relaxation time by the Eq. (3.6). We have plotted the drag coefficient as a function of temperature. Drag coefficient accounts for average momentum change and it increases with system

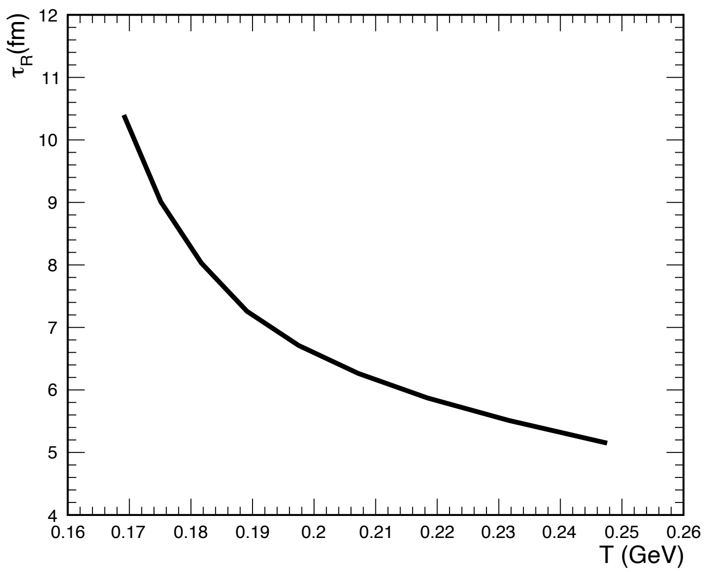

Figure 4.1: Variation of relaxation time with temperature

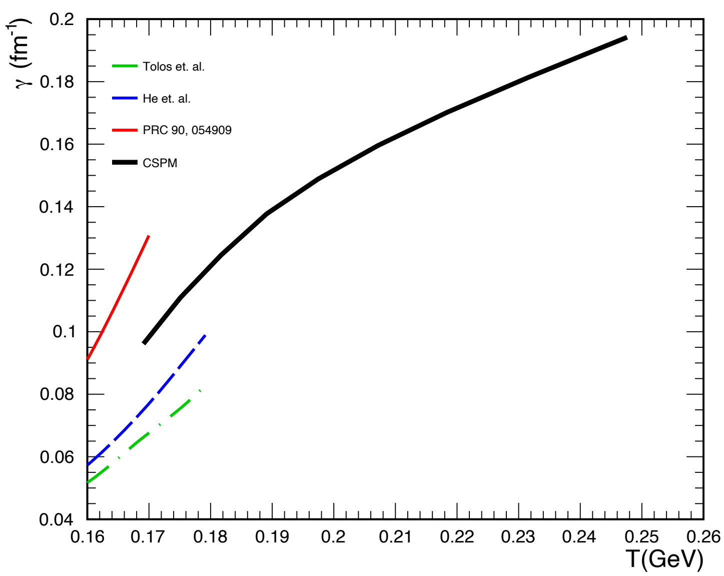

Figure 4.2: Variation of drag coefficient with temperature compared with results from [25].

temperature. This is due to the fact that, when the system is denser, the charm quark will endure higher drag force. We have observed that our results follow the same trend as the result from [25] in which the authors have estimated drag coefficient for hadron gas while we have calculated for charm quarks in QGP.

We have also estimated the momentum diffusion coefficient using Einstein's relation (3.7). The momentum diffusion coefficient accounts for the broadening of the momentum distribution of charm quarks. It shows an increasing trend with temperature which implies that for a system at a higher temperature, i.e. central heavy-ion collision, momentum diffusion is higher.

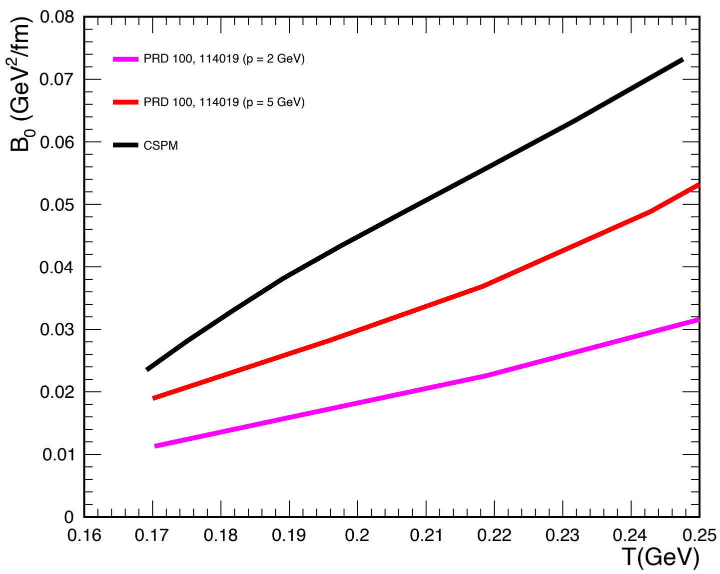

Figure 4.3: Variation of momentum diffusion coefficient with temperature

Our results agree to quite a good extent with results from [26].

Finally, Spatial diffusion coefficient has been estimated using (3.8) We

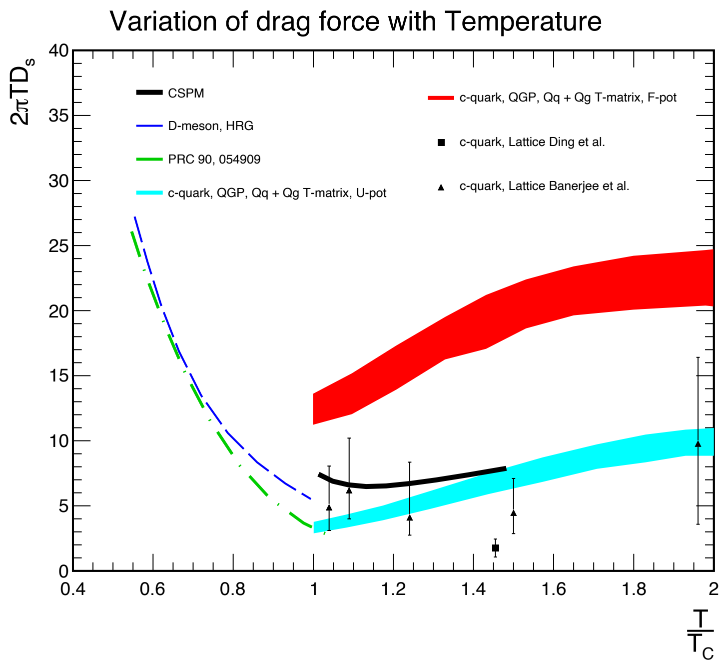

Figure 4.4: Variation of spatial diffusion coefficient with temperature

have plotted, $2\pi TD_s$, as a function of initial temperature. From the plot (4.4), we can study the phase transition of the system. We can observe a minimum around the hadronization temperature which marks a phase transition. We have compared our results with several other works [24, 25, 27, 28, 29], all of them show the same trend. Refs. [27, 28] have been done for hadron gas that shows a decreasing trend while Refs. [24, 25, 29] have estimated spatial diffusion coefficient for QGP medium by taking various approaches which show an increasing trend beyond the critical temperature. According to AdS/CFT calculation, the minimum value for $2\pi TD_s$ is ~ 1 [30]. We can observe that the spatial diffusion coefficient decreases with temperature, reaches a minimum, and then increases with temperature. The same trend can be observed when the shear viscosity to entropy density ratio is plotted with temperature.

From all the above plots, we can conclude that the result obtained from the Color string percolation model agrees to a very good extent with that obtained by other models for the hadronic system or QGP medium.

Chapter 5

Conclusions

In this thesis, we have studied the systems produced in relativistic high energy collision using the Color string percolation model. Many observables, like temperature, shear viscosity to entropy density ratio, mean free path, etc can be estimated using this model. We have studied the diffusion of charm quark in the QGP medium. This enables us to understand the QGP medium better and predict its properties.

We have studied the following in this thesis:

1. We estimated the temperature of the system produced in the relativistic heavy-ion collision. We found that around the critical percolation density $\xi_c = 1.2$, the estimated temperature is 0.167 GeV, which is in the range of hadronization temperature calculated by other models.

2. We have estimated relaxation time for charm quarks in a deconfined medium using CSPM.

3. The drag coefficient obtained from CSPM is found to be in good agree-

ment with other results[25]. As the temperature and system density increases the drag coefficient increases with it.

4. We have studied the variation of transverse momentum diffusion coefficient with temperature. The increasing momentum diffusion coefficient shows that, at a higher temperature, the momentum spectra becomes broader.

5. We have estimated the spatial diffusion coefficient and plotted it against temperature. A change in trend can be seen near critical temperature which suggests a possible phase transition.

Relatively, the study of heavy quarks in the QGP medium is a new and challenging domain that offers interesting answers. It is an excellent probe for investigating the QGP medium.

Bibliography

[1] http://qgp-data.phy.duke.edu

[2] B. Mohanty, PoS **CPOD2013**, 001 (2013).

[3] https://particlesandfriends.wordpress.com/2016/10/14/evolution-of-collisions-and-qgp

[4] D. Sahu and R. Sahoo, [arXiv:2006.04185 [hep-ph]]

[5] H. Satz, Lect. Notes Phys. **841**, 1 (2012).

[6] R. P. Scharenberg, B. K. Srivastava and C. Pajares, Phys. Rev. D **100**, 114040 (2019).

[7] M. A. Braun and C. Pajares, Eur. Phys. J. C **16**, 349 (2000).

[8] B. K. Srivastava *et al.* [STAR], Nukleonika **51S3**, S109 (2006).

[9] M. A. Braun, F. del Moral and C. Pajares, Nucl. Phys. A **715**, 791 (2003).

[10] C.Y.Wong, Introduction to high energy heavy ion collisions, 289 (1994).

[11] J. S. Schwinger, Phys. Rev. **128**, 2425 (1962).

[12] A. Bialas, Phys. Lett. B **466**, 301 (1999).

[13] J. Dias de Deus and C. Pajares, Phys. Lett. B **642**, 455 (2006).

[14] R. P. Scharenberg, B. K. Srivastava and A. S. Hirsch, Eur. Phys. J. C **71**, 1510 (2011).

[15] F. Becattini, P. Castorina, A. Milov and H. Satz, Eur. Phys. J. C **66**, 377 (2010).

[16] P. Kovtun, D. T. Son and A. O. Starinets, Phys. Rev. Lett. **94**, 111601 (2005).

[17] D. Kazakov, Phys. Usp. **57**, 930 (2014).

[18] M. Kurian, M. Singh, V. Chandra, S. Jeon and C. Gale, Phys. Rev. C **102**, 044907 (2020).

[19] U. W. Heinz, Nucl. Phys. A **721**, 30 (2003).

[20] P. Foka and M. A. Janik, Rev. Phys. **1**, 154 (2016).

[21] J. M. Torres-Rincon, L. M. Abreu, D. Cabrera, F. J. Llanes-Estrada and L. Tolos, J. Phys. Conf. Ser. **503**, 012020 (2014).

[22] R. Rapp and H. van Hees, [arXiv:0803.0901 [hep-ph]].

[23] P. Petreczky and D. Teaney, Phys. Rev. D **73**, 014508 (2006).

[24] L. Tolos and J. M. Torres-Rincon, Phys. Rev. D **88**, 074019 (2013).

[25] V. Ozvenchuk, J. M. Torres-Rincon, P. B. Gossiaux, L. Tolos and J. Aichelin, Phys. Rev. C **90**, 054909 (2014).

[26] B. Singh, A. Abhishek, S. K. Das and H. Mishra, Phys. Rev. D **100**, 114019 (2019).

[27] D. Banerjee, S. Datta, R. Gavai and P. Majumdar, Phys. Rev. D **85**, 014510 (2012).

[28] H. T. Ding, A. Francis, O. Kaczmarek, F. Karsch, H. Satz and W. Soldner, J. Phys. G **38**, 124070 (2011).

[29] Y. Akiba, A. Angerami, H. Caines, A. Frawley, U. Heinz, B. Jacak, J. Jia, T. Lappi, W. Li and A. Majumder, *et al.* [arXiv:1502.02730 [nucl-ex]].

[30] P. Kovtun, D. T. Son and A. O. Starinets, JHEP **10**, 064 (2003).